

Extension of Minimal Fermionic Dark Matter Model

Amit Dutta Banik ¹, Debasish Majumdar ²

*Astroparticle Physics and Cosmology Division,
Saha Institute of Nuclear Physics,
1/AF Bidhannagar, Kolkata 700064, India*

Abstract

We explore a fermionic dark matter model with a possible extension of Standard Model (SM) of particle physics into two Higgs doublet model. Higgs doublets couple to the singlet fermionic dark matter through a non renormalizable coupling predicting a new physics scale. We show the viability of such dark matter candidate by calculating the direct detection cross-section and relic density and comparing them with experimentally obtained results.

1 Introduction

The satellite borne experiments like Planck, WMAP etc. which study the anisotropies of cosmic microwave background radiations predict that around more than a quarter of the constituents of the universe is made of unknown dark matter. The recent Planck data suggest that the relic abundance for dark matter is within the range $\Omega_{DM}h^2 = 0.1199 \pm 0.0027$ [1], where h is the Hubble parameter normalised to $100 \text{ km s}^{-1} \text{ Mpc}^{-1}$. There are also several ongoing terrestrial experiments for direct detection of dark matter. Although no dark matter is convincingly detected but there are recent claims of the observance of three potential dark matter signals by CDMS direct dark matter search experiment [2]. Earlier the DAMA/NAI dark matter direct search experiment also claimed to have observed the signature of the annual modulation of dark matter signal – a phenomenon that the dark matter direct search signal should exhibit due to the revolution of earth around the sun. The ongoing direct search experiments give an upper bound in $\sigma_{\text{scat}} - m_\chi$ plane where σ_{scat} is the dark matter elastic scattering cross-sections off the target detector nucleon and m_χ is the dark matter mass. Dark matter particles can also be trapped in a highly gravitating astrophysical objects and eventually undergo annihilation to produce γ 's or fermion anti-fermion pairs. Such events should show up as excesses over the expected abundance of the particles in the cosmos (for instance in cosmic rays). Indirect searches of dark matter by detecting their annihilation products can be realised by looking for such excesses in the universe.

¹email: amit.duttabanik@saha.ac.in

²email: debasish.majumdar@saha.ac.in

In fact the satellite borne experiments like Fermi-Lat [3], AMS [4] or the earth bound experiments like H.E.S.S. [5], MAGIC [6] and also the Antarctica balloon-borne experiments like ATIC [7] look for gamma ray, positron or antimatter excesses.

Although the dark matter (DM) searches are being vigorously pursued, the particle constituent of dark matter is not known at all. Various particle physics models for cold dark matter (CDM) are available in literature that include the popular candidate neutralino which is supersymmetry motivated, Kaluza Klein dark matter from theories of extra dimensions or other proposed theories from simple extensions of standard model (like adding a scalar singlet or an inert doublet and then imposing a discrete Z_2 symmetry that ensures the stability of the dark matter candidate) [8]. In this work we propose a new particle candidate for dark matter where we consider Two Higgs Doublet Model (THDM) [9], and add a singlet fermion to the model. The dark matter candidate in this model is the singlet fermion. We then explore the viability of this singlet fermion for being a candidate for cold dark matter in the framework of THDM.

In a previous work [10], a minimal model of fermionic singlet dark matter is proposed, where a fermion Lagrangian is added to the Standard Model Lagrangian. In this work however, we propose a new fermionic dark matter model in the framework of THDM. The stability of such a dark matter is ensured by assigning the baryon and lepton charge of the singlet fermion to be zero and the baryon and lepton number is conserved. Also a discrete symmetry is introduced between the Higgs doublets of THDM to avoid flavour changing neutral current (FCNC) processes [11]. The singlet fermion, the DM candidate in the present model, couples to both the higgs doublets through a dimension five coupling when a new physics scale Λ is introduced. In this work we explore the possibility that within the framework of this model, the fermion (added to the THDM) is a viable candidate for cold dark matter. We evaluate its direct detection cross-section, relic density and explore how the proposed fermionic candidate affects the collider bounds of THDM. We organise the paper as follows. In Section 2, we give the model and describe the model parameters. The aspect of possible collider physics phenomenology for the model is addressed in Section 3. In Section 4 we calculate the relic density of the dark matter candidate in our proposed model. The model parameters are constrained by comparing the calculated relic density with observational dark matter relic density data obtained from Planck/WMAP experiments. In Section 5, we calculate the spin independent direct detection scattering cross-section for the present dark matter candidate for different masses of dark matter. The model parameters are then further constrained by results obtained from dark matter direct detection experiments. Finally some concluding remarks and discussions are given in Section 6.

2 The Model

In the present work we add a singlet fermion with two Higgs doublet model. The singlet fermion χ in the resulting model, is the proposed candidate for dark matter. The Lagrangian for χ can be written as

$$\mathcal{L}_\chi = \bar{\chi} i \gamma^\mu \partial_\mu \chi - m \bar{\chi} \chi . \quad (1)$$

In order to ensure the stability of χ , the dark matter candidate in the present singlet fermion dark matter (FDM) model, we assign zero baryon number and zero lepton number to the singlet fermion and assume baryon number and lepton number to be conserved [10].

The total Lagrangian of the model can be written as

$$\mathcal{L} = \mathcal{L}_{\text{THDM}} + \mathcal{L}_{\chi} + \mathcal{L}_{\text{int}} \quad (2)$$

where \mathcal{L}_{int} denotes the interaction Lagrangian. The two higgs doublet model is the most general non supersymmetric extension of Standard Model (SM) when another complex doublet of same hypercharge is added. The two higgs doublet model potential is expressed as

$$\begin{aligned} V(\Phi_1, \Phi_2) = & m_1^2 \Phi_1^\dagger \Phi_1 + m_2^2 \Phi_2^\dagger \Phi_2 + (m_{12}^2 \Phi_1^\dagger \Phi_2 + \text{h.c.}) + \frac{1}{2} \lambda_1 (\Phi_1^\dagger \Phi_1)^2 + \frac{1}{2} \lambda_2 (\Phi_2^\dagger \Phi_2)^2 \\ & + \lambda_3 (\Phi_1^\dagger \Phi_1)(\Phi_2^\dagger \Phi_2) + \lambda_4 (\Phi_1^\dagger \Phi_2)(\Phi_2^\dagger \Phi_1) + \frac{1}{2} \lambda_5 [(\Phi_1^\dagger \Phi_2)^2 + \text{h.c.}] , \end{aligned} \quad (3)$$

where both the doublet fields have non zero vacuum expectation values and a discrete symmetry (Z_2) is imposed in between the doublet fields in order to avoid FCNC processes. We consider a CP conserving two Higgs doublet model potential where all the parameters expressed in Eq. 3 are assumed to be real. In addition, the imposed discrete symmetry Z_2 will result in mainly four types of THDM namely type I, type II, lepton specific and flipped THDM depending on the coupling of fermions with the doublet fields. All the mentioned models will give rise to two charged Higgs fields (H^\pm), two CP even scalar fields (h, H), one CP odd scalar (A) and three Goldstone bosons (G^\pm, G). The Higgs doublets Φ_1 and Φ_2 expressed in terms of physical states of the particles are written as [9],

$$\Phi_1 = \begin{pmatrix} c_\beta G^+ - s_\beta H^+ \\ \frac{1}{\sqrt{2}}(v_1 + c_\alpha H - s_\alpha h + i c_\beta G - i s_\beta A) \end{pmatrix} \quad (4)$$

$$\Phi_2 = \begin{pmatrix} s_\beta G^+ + c_\beta H^+ \\ \frac{1}{\sqrt{2}}(v_2 + s_\alpha H + c_\alpha h + i s_\beta G + i c_\beta A) \end{pmatrix}, \quad (5)$$

where $\tan \beta (= \frac{v_2}{v_1})$, is the ratio of the vacuum expectation values of both doublets and α is the measure of mixing between two CP even scalars. The terms c_x and s_x ($x = \alpha, \beta$) denote $\cos x$ and $\sin x$ respectively.

The interaction Lagrangian, \mathcal{L}_{int} of dark matter fermion (Eq. 2) with Φ_1 and Φ_2 doublet fields is given by

$$\mathcal{L}_{\text{int}} = -\frac{g_1}{\Lambda} (\Phi_1^\dagger \Phi_1) \bar{\chi} \chi - \frac{g_2}{\Lambda} (\Phi_2^\dagger \Phi_2) \bar{\chi} \chi, \quad (6)$$

where Λ is a high energy scale. Interaction of THDM sector with the DM candidate can be obtained easily from Eqs. 2-6. Without any loss of generality we assume both the Higgs fields couple equivalently to DM fermion. With this assumption we have $g_1 = g_2 = g_c$ in Eq. 6. Thus the necessary couplings of DM to Higgs particles h and H take the form

$$g_{\bar{\chi}\chi h} = g_0 \sin(\beta - \alpha), \quad g_{\bar{\chi}\chi H} = g_0 \cos(\beta - \alpha) \quad (7)$$

and

$$g_0 = g_c \frac{v}{\Lambda} . \quad (8)$$

The interaction Lagrangian, \mathcal{L}_{int} in Eq. 6 also contains the quartic terms involving the DM fermions χ and the fields h , H , A and H^+ . The corresponding couplings are given by

$$g_{\bar{\chi}\chi hh} = \frac{g_c}{2\Lambda}, \quad g_{\bar{\chi}\chi HH} = \frac{g_c}{2\Lambda}, \quad g_{\bar{\chi}\chi AA} = \frac{g_c}{2\Lambda}, \quad \text{and} \quad g_{\bar{\chi}\chi H^+ H^-} = \frac{g_c}{\Lambda} . \quad (9)$$

Mass of the singlet fermion comes out to be

$$M = m_0 + \frac{g_1}{2\Lambda} v_1^2 + \frac{g_2}{2\Lambda} v_2^2$$

Following the simplified assumption ($g_1 = g_2 = g_c$) and using Eq. 8, fermion mass turns out to be

$$M = m_0 + \frac{g_0}{2} v \quad (10)$$

where $v = \sqrt{v_1^2 + v_2^2}$, is 246 GeV. As seen the new physics scale Λ determines the coupling of DM particle to THDM sector and contributes significantly to the singlet fermion mass. From Eq. 9 we can easily conclude that quartic couplings of dark matter to the Higgs sector are smaller with respect to the couplings expressed in Eq. 7.

As mentioned, the discrete Z_2 symmetry imposed between the Higgs doublets will result in four different types of THDM. In this work we consider THDM of type I and type II. In type I THDM only one scalar doublet (say Φ_2) couples to the SM particles whereas in type II THDM, up type quarks couple to one Higgs doublet and down type quarks and leptons couple to the other. Higgs couplings to up type quarks, down type quarks and leptons in case of type I THDM are given as [11]

$$g_{\bar{f}ffh} = -i \frac{gm_f}{2M_W} \frac{\cos \alpha}{\sin \beta} \quad g_{\bar{f}fH} = -i \frac{gm_f}{2M_W} \frac{\sin \alpha}{\sin \beta} , \quad (11)$$

where f denotes all SM fermions (up quarks, down quarks and leptons) respectively. In case of type II THDM, Yukawa couplings are

$$\begin{aligned} g_{\bar{u}uh} &= -i \frac{gm_u}{2M_W} \frac{\cos \alpha}{\sin \beta} & g_{\bar{u}uH} &= -i \frac{gm_u}{2M_W} \frac{\sin \alpha}{\sin \beta} , \\ g_{\bar{d}dh} &= -i \frac{gm_d}{2M_W} \frac{-\sin \alpha}{\cos \beta} & g_{\bar{d}dH} &= -i \frac{gm_d}{2M_W} \frac{\cos \alpha}{\cos \beta} , \\ g_{\bar{l}lh} &= -i \frac{gm_l}{2M_W} \frac{-\sin \alpha}{\cos \beta} & g_{\bar{l}lH} &= -i \frac{gm_l}{2M_W} \frac{\cos \alpha}{\cos \beta} . \end{aligned} \quad (12)$$

In the above u corresponds to up type quarks (u, c, t), d corresponds to down type quarks (d, s, b) and l represents three families of leptons (e, μ, τ) respectively.

Couplings to the gauge bosons ($V = W, Z$) for THDM I and THDM II are same and given by [11]

$$\begin{aligned} g_{WW h} &= igM_W \sin(\beta - \alpha) g^{\mu\nu} & g_{WW H} &= igM_W \cos(\beta - \alpha) g^{\mu\nu} \\ g_{ZZ h} &= ig \frac{M_Z}{\cos \theta_W} \sin(\beta - \alpha) g^{\mu\nu} & g_{ZZ H} &= ig \frac{M_Z}{\cos \theta_W} \cos(\beta - \alpha) g^{\mu\nu} \end{aligned} \quad (13)$$

In Eqs. 11-13, m_x ($x = u, d, l$ etc) represents the mass of quarks or leptons and M_W and M_Z denote the masses of W and Z bosons respectively. In the present work, for type I and type II THDM, we consider h to be SM like Higgs boson with mass 125 GeV.

3 Collider physics phenomenology

The existence of a scalar boson of mass 125 GeV has been confirmed by Large Hadron Collider (LHC) [12, 13]. In this work we treat the new found scalar boson to be equivalent to one of the CP even scalars (h) appearing in THDMs. We further extend the model by including a possible fermionic dark matter candidate. This will necessarily affect the phenomenology of collider physics. If the dark matter mass is small ($M \leq m_h/2$) then one would expect an invisible decay of SM like Higgs boson (h) and the total decay width will change depending on the coupling constant $g_{\tilde{\chi}\chi h}$ and other THDM parameters α, β . Since both the scalar bosons couple to the DM fermion in the present framework, it is likely to expect a considerable change in the standard bounds on THDM sector as predicted by recent studies. The signal strength of SM like Higgs boson (h) to a specific channel for type I and type II THDM are given by [14]

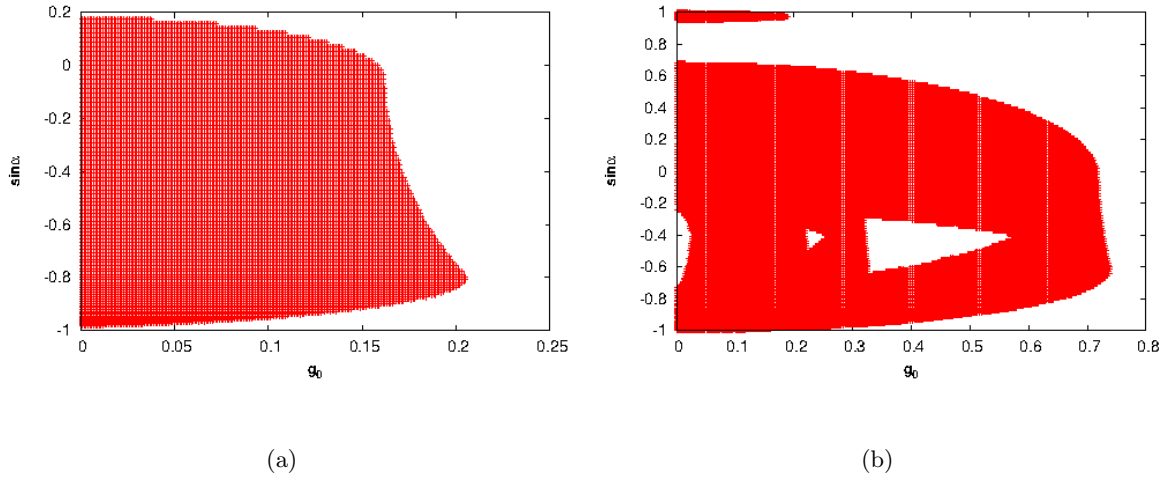


Figure 1: Allowed $g_0 - \sin \alpha$ parameter space for Higgs to diphoton decay in THDM I + FDM model for $R'_I = 1.0$ (a), and $R'_I = 0.5$ (b)

$$R_I = \frac{\cos^2 \alpha}{\sin^2 \beta} \frac{\text{BR}^{\text{THDM}}}{\text{BR}^{\text{SM}}} \quad R_{II} = \frac{9.53 f_t^2 + 0.083 f_b^2 + 0.36 f_t f_b}{9.25} \frac{\text{BR}^{\text{THDM}}}{\text{BR}^{\text{SM}}} \quad (14)$$

where $f_t = \frac{\cos \alpha}{\sin \beta}$ and $f_b = \frac{-\sin \alpha}{\cos \beta}$ and BR^{D} ($\text{D} \equiv \text{THDM or SM as the case may be}$) denotes the branching ratio to a specific channel neglecting the contribution from charged bosons. The modified signal strength for THDM type I and THDM type II in presence of a fermionic dark matter of mass

$M \leq m_h/2$ is written as

$$R'_I = \frac{\cos^2 \alpha}{\sin^2 \beta} \frac{\text{BR}^{\text{THDM+FDM}}}{\text{BR}^{\text{SM}}} \quad R'_{II} = \frac{9.53f_t^2 + 0.083f_b^2 + 0.36f_t f_b}{9.25} \frac{\text{BR}^{\text{THDM+FDM}}}{\text{BR}^{\text{SM}}} \quad (15)$$

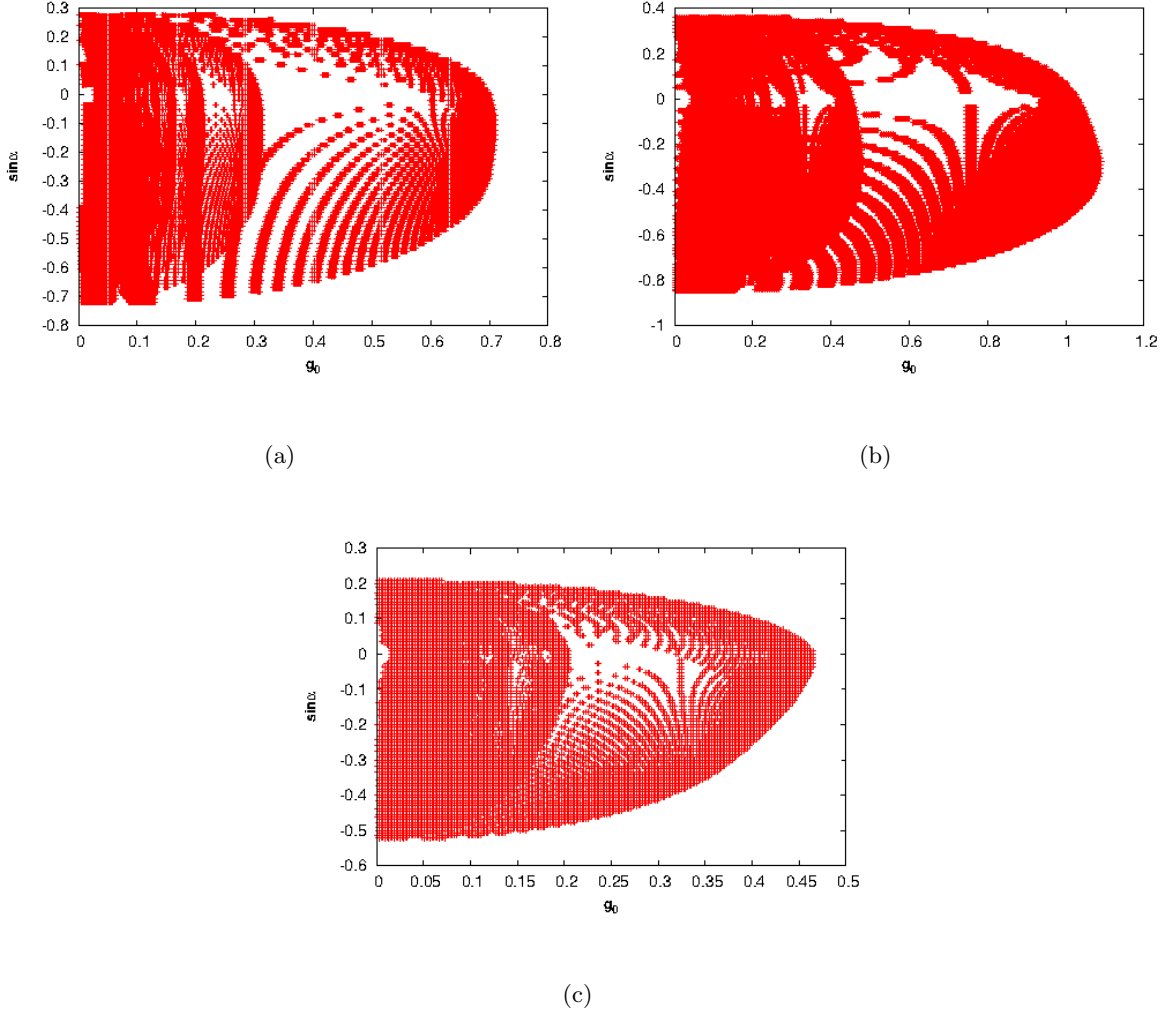


Figure 2: Allowed $g_0 - \sin \alpha$ parameter space for Higgs to diphoton decay in THDM II + FDM model for $R'_{II} = 1.0$ (a), $R'_{II} = 0.5$ (b) and $R'_{II} = 2.0$ (c)

CMS and ATLAS independently observed the signal strength for $h \rightarrow \gamma\gamma$ channel [15]. The modified signal strengths expressed in Eq. 15, as stated earlier will depend on THDM parameters α, β and the DM- h coupling $g_{\tilde{\chi}\chi h}$ respectively and will constrain these parameters. The expression of DM- h coupling obtained from Eq. 7 indicates that the signal strength will effectively depend on α, β and g_0 . In Fig. 1a we present the allowed region of $g_0 - \sin \alpha$ parameter space for THDM I + FDM with $1 \leq \tan \beta \leq 20$

values in the SM limit ($R'_I = 1.0$) whereas Fig. 1b shows similar region for $R'_I = 0.5$. It can be seen from Fig. 1 that for the latter case allowed parameter space increases significantly. In Fig. 2(a-c) we plot the same for THDM II + FDM model for three different values of R'_{II} , given as $R'_{II} = 1.0, 0.5, 2.0$. In case of THDM II + FDM model the allowed region of $g_0 - \sin \alpha$ parameter space is reduced as the signal strength (R'_{II}) becomes greater than unity. For low mass DM ($M \leq m_h/2$), Higgs to diphoton signal strength will also set an upper bound on g_0 and DM mass. In Fig. 3 we present the exclusion limits on DM mass M ($M \leq m_h/2$) and g_0 for THDM I + FDM and THDM II + FDM. The red lines appearing in the Fig. 3(a), 3(b) represent the bounds for the case $R'_{I/II} = 1.0$ whereas the green lines are the same for $R'_{I/II} = 0.5$ for both THDM I + FDM and THDM II + FDM models. The blue line appearing in Fig. 3b represents the case for $R'_{II} = 2.0$ when we consider THDM II + FDM model. The area below each of the curves is favoured for the respective cases mentioned above by the Higgs to $\gamma\gamma$ constraints measured using Eq. 15, whereas the area above each of those curves (red and green for THDM I + FDM, red, blue and green for THDM II + FDM) are not allowed by the $h \rightarrow \gamma\gamma$ constraints mentioned above. It can be easily observed from the plots in Fig. 3 that for $R'_{I/II} = 0.5$ the upper bound on g_0 is relaxed in comparison with the same for $R'_{I/II} = 1.0$. It is also seen from Fig. 3 for $R'_{II} = 2.0$, the bound on g_0 is more constrained (blue line in Fig. 3b) than for $R'_{II} = 1.0$. All the exclusion plots show a similar nature and maximum attainable value of g_0 (g_0^{max}) remains almost constant for low mass region independent of the choice of $R'_{I/II}$ values. It then starts increasing with the increase in DM mass. As DM mass approaches $m_h/2$ – the Higgs pole region – upper limit on g_0 is relaxed and it can attain value $\simeq 1$. Since $g_{\tilde{\chi}\chi h} = g_0 \sin(\beta - \alpha)$, it is likely to conclude that g_0 is also the upper bound of the $g_{\tilde{\chi}\chi h}$ coupling in the SM limit when $\sin(\beta - \alpha) = 1$.

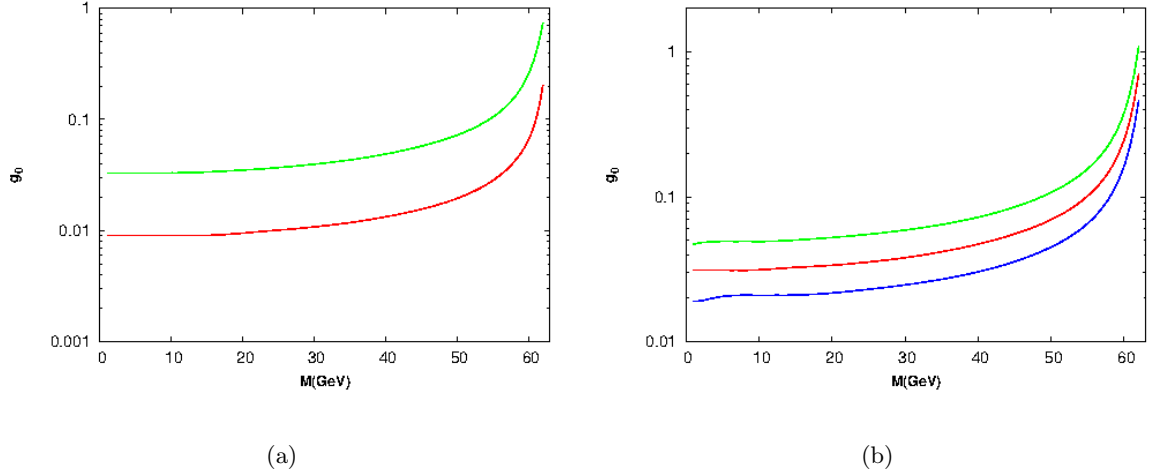


Figure 3: Bound on dark matter mass M and g_0 obtained from h to $\gamma\gamma$ constraints

However, for the case when DM candidate is massive ($M > m_h/2$), then there would not be any significant change in the THDM parameter space as the decay of SM like Higgs to DM will be disallowed

kinematically. Hence, for $M > m_h/2$ the allowed range of parameter space is independent of the coupling g_0 and will be constrained by THDM parameters α, β [16].

4 DM annihilation and relic density

In order to evaluate the relic density of the fermionic dark matter candidate proposed in this work one needs to solve the Boltzmann equation [17]

$$\frac{dn}{dt} + 3Hn = -\langle\sigma v\rangle(n^2 - n_{eq}^2) \quad (16)$$

where n is the actual number density of the particle species, H is the Hubble parameter and n_{eq} is the number density at thermal equilibrium. An approximate expression for relic density Ω or Ωh^2 ($h = H/(100 \text{ kms}^{-1} \text{ Mpc}^{-1})$) that can be obtained from Eq. 16 is given by

$$\Omega_{DM} h^2 = \frac{1.07 \times 10^9 x_F}{\sqrt{g_*} M_{Pl} \langle\sigma v\rangle} \quad (17)$$

where $x_F = M/T_F$, g_* is effective degrees of freedom and $M_{Pl} = 1.22 \times 10^{19}$ is the Planck mass.

The particle physics input to Eqs. 16,17 is the thermal averaged annihilation cross-section $\langle\sigma v\rangle$ and one needs to calculate this quantity for the present fermionic dark matter candidate in our model. Also it is required to evaluate the freeze out temperature T_F for the species considered here in order to compute the relic density given in Eq. 17. The freeze out temperature T_F is determined from the iterative solution of the equation

$$x_F = \ln \left(\frac{M}{2\pi^3} \sqrt{\frac{45 M_{Pl}^2}{2g_* x_F} \langle\sigma v\rangle} \right). \quad (18)$$

It is therefore essential to calculate the the annihilation cross-section of the dark matter candidate. The freeze out temperature thus obtained is then used to evaluate the relic density.

Dark matter candidates in the present model annihilate to SM particles through h or H since quartic interactions are small and their contribution to annihilation are negligible. The total annihilation cross-section σv can be expressed as a sum of the three terms

$$\begin{aligned} \sigma v = (s - 4M^2) & \left[A \frac{1}{(s - m_h^2)^2 + m_h^2 \Gamma_h^2} + B \frac{1}{(s - m_H^2)^2 + m_H^2 \Gamma_H^2} \right. \\ & \left. + C \frac{2(s - m_h^2)(s - m_H^2) + 2m_h m_H \Gamma_h \Gamma_H}{[(s - m_h^2)^2 + m_h^2 \Gamma_h^2][(s - m_H^2)^2 + m_H^2 \Gamma_H^2]} \right]. \end{aligned} \quad (19)$$

In Eq. 19, Γ_h and Γ_H are decay widths of light Higgs (h) and heavy Higgs particle (H) respectively. We set the light Higgs mass m_h to be 125 GeV and the heavy Higgs mass m_H is assumed to be 360 GeV in this work. These values are consistent with recent bounds on THDM sector [16]. The terms

A , B and C in the expression for σv (Eq. 19) in case of THDM I are given as

$$A = g_{\bar{\chi}\chi h}^2 \frac{G_F}{4\pi\sqrt{2}} \left[\frac{c_\alpha^2}{s_\beta^2} (N_c m_{u_i}^2 \gamma_{u_i}^3 + N_c m_{d_i}^2 \gamma_{d_i}^3 + m_{l_i}^2 \gamma_{l_i}^3) + \frac{1}{2} s_{\beta-\alpha}^2 s (1 - x_W + \frac{3}{4} x_W^2) \gamma_W + \frac{1}{4} s_{\beta-\alpha}^2 s (1 - x_Z + \frac{3}{4} x_Z^2) \gamma_Z \right], \quad (20)$$

$$B = g_{\bar{\chi}\chi H}^2 \frac{G_F}{4\pi\sqrt{2}} \left[\frac{s_\alpha^2}{s_\beta^2} (N_c m_{u_i}^2 \gamma_{u_i}^3 + N_c m_{d_i}^2 \gamma_{d_i}^3 + m_{l_i}^2 \gamma_{l_i}^3) + \frac{1}{2} c_{\beta-\alpha}^2 s (1 - x_W + \frac{3}{4} x_W^2) \gamma_W + \frac{1}{4} c_{\beta-\alpha}^2 s (1 - x_Z + \frac{3}{4} x_Z^2) \gamma_Z \right], \quad (21)$$

and

$$C = g_{\bar{\chi}\chi h} g_{\bar{\chi}\chi H} \frac{G_F}{4\pi\sqrt{2}} \left[\frac{c_\alpha s_\alpha}{s_\beta^2} (N_c m_{u_i}^2 \gamma_{u_i}^3 + N_c m_{d_i}^2 \gamma_{d_i}^3 + m_{l_i}^2 \gamma_{l_i}^3) + \frac{1}{2} s_{\beta-\alpha} c_{\beta-\alpha} s (1 - x_W + \frac{3}{4} x_W^2) \gamma_W + \frac{1}{4} s_{\beta-\alpha} c_{\beta-\alpha} s (1 - x_Z + \frac{3}{4} x_Z^2) \gamma_Z \right]. \quad (22)$$

For THDM type II, the expressions for A , B and C are

$$A = g_{\bar{\chi}\chi h}^2 \frac{G_F}{4\pi\sqrt{2}} \left[N_c m_{u_i}^2 \frac{c_\alpha^2}{s_\beta^2} \gamma_{u_i}^3 + N_c m_{d_i}^2 \frac{s_\alpha^2}{c_\beta^2} \gamma_{d_i}^3 + m_{l_i}^2 \frac{s_\alpha^2}{c_\beta^2} \gamma_{l_i}^3 + \frac{1}{2} s_{\beta-\alpha}^2 s (1 - x_W + \frac{3}{4} x_W^2) \gamma_W + \frac{1}{4} s_{\beta-\alpha}^2 s (1 - x_Z + \frac{3}{4} x_Z^2) \gamma_Z \right], \quad (23)$$

$$B = g_{\bar{\chi}\chi H}^2 \frac{G_F}{4\pi\sqrt{2}} \left[N_c m_{u_i}^2 \frac{s_\alpha^2}{s_\beta^2} \gamma_{u_i}^3 + N_c m_{d_i}^2 \frac{c_\alpha^2}{c_\beta^2} \gamma_{d_i}^3 + m_{l_i}^2 \frac{c_\alpha^2}{c_\beta^2} \gamma_{l_i}^3 + \frac{1}{2} c_{\beta-\alpha}^2 s (1 - x_W + \frac{3}{4} x_W^2) \gamma_W + \frac{1}{4} c_{\beta-\alpha}^2 s (1 - x_Z + \frac{3}{4} x_Z^2) \gamma_Z \right], \quad (24)$$

$$C = g_{\bar{\chi}\chi h} g_{\bar{\chi}\chi H} \frac{G_F}{4\pi\sqrt{2}} \left[N_c m_{u_i}^2 \frac{s_\alpha}{s_\beta} \frac{c_\alpha}{s_\beta} \gamma_{u_i}^3 - N_c m_{d_i}^2 \frac{c_\alpha}{c_\beta} \frac{s_\alpha}{c_\beta} \gamma_{d_i}^3 - m_{l_i}^2 \frac{c_\alpha}{c_\beta} \frac{s_\alpha}{c_\beta} \gamma_{l_i}^3 + \frac{1}{2} c_{\beta-\alpha} s_{\beta-\alpha} s (1 - x_W + \frac{3}{4} x_W^2) \gamma_W + \frac{1}{4} c_{\beta-\alpha} s_{\beta-\alpha} s (1 - x_Z + \frac{3}{4} x_Z^2) \gamma_Z \right]. \quad (25)$$

In all the above expressions $\gamma_a = (1 - \frac{4m_a^2}{s})^{\frac{1}{2}}$ ($a = u, d, l$ etc.) and $N_c = 3$ for quarks. Thermal average of pair annihilation cross-section of DM to SM particles is given by

$$\langle \sigma v \rangle = \frac{1}{8M^4 T_F K_2^2(M/T_F)} \int_{4M^2}^{\infty} ds \sigma(s) (s - 4M^2) \sqrt{s} K_1(\sqrt{s}/T_F), \quad (26)$$

where K_1 and K_2 are modified Bessel functions and T_F is the freeze out temperature of the DM candidate.

Using Eqs. 19 - 26, the annihilation cross-section $\langle\sigma v\rangle$ are evaluated for both the THDM I + FDM and THDM II + FDM models. The model parameters g_0 , α and β are varied for different dark matter masses to obtain $\langle\sigma v\rangle$ in order to solve Eq. 18 iteratively and subsequently obtain the relic densities using Eq. 17 for each set of choice of parameters. The range of parameters are initially chosen from the $g_0 - \sin\alpha$ parameter space of $h \rightarrow \gamma\gamma$ decay for both the THDM I + FDM and THDM II + FDM models as discussed in Section 3 and shown in Figs. 1, 2 for the chosen range of $\tan\beta$. As mentioned earlier, for $M > m_h/2$ the branching ratio of SM like Higgs boson is same as that of THDM's and hence the bounds on type I and type II THDM will remain invariant in this scenario. Parameters α and β are highly constrained from the experimental bounds on THDM sector [16]. On the other hand for $M \leq m_h/2$, we use the allowed parameter space obtained from the collider phenomenology of Higgs to diphoton discussed in Section 3. The range of β is also fixed by $1 \leq \tan\beta \leq 20$ as chosen in Section 3.

The calculated relic densities are then compared with Planck experimental results for relic density. Thus we constrain the parameters of our model which in fact give the allowed THDM parameters and also the couplings of the chosen fermionic dark matter candidate. We thus obtain the parameter values for different dark matter masses allowed by Planck relic density data.

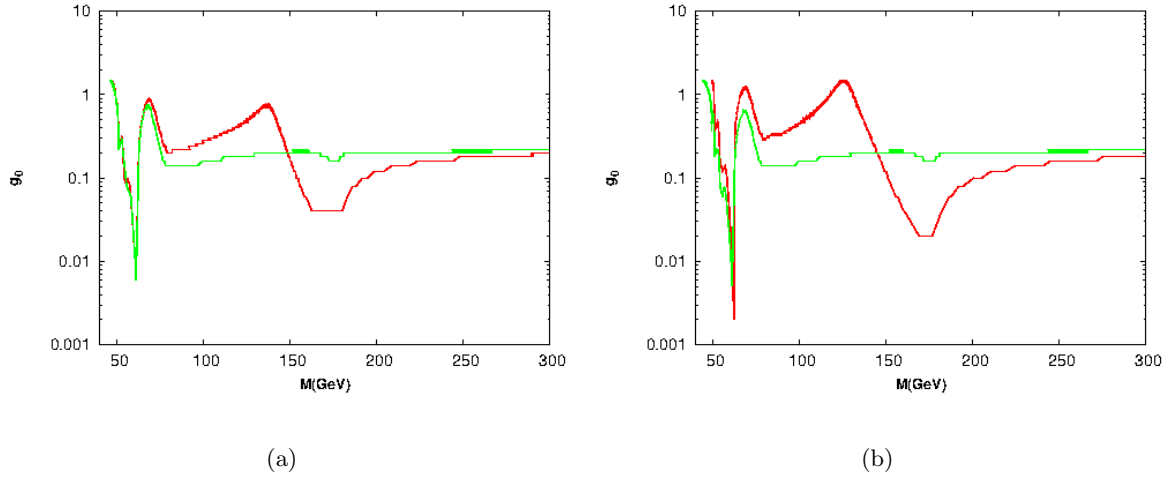


Figure 4: DM mass M vs g_0 satisfying relic density of DM for THDM I + FDM and THDM II + FDM

In Fig. 4 we plot g_0 for different values of the fermionic dark matter mass M . All plotted values of g_0 and M are allowed by Planck relic density data. The plots are shown for two sets of α , β values. In one case, the chosen set ($\alpha = -30$, $\beta = 65$) is same for both the models while other two different sets, ($\alpha = 10$, $\beta = 65$) and ($\alpha = 20$, $\beta = 65$) are chosen for the models THDM I + FDM and THDM II + FDM respectively. The assumed α , β values in the plots satisfy $h \rightarrow \gamma\gamma$ bounds discussed in Section 3 (for both the cases $M \leq m_h/2$ and $M > m_h/2$) and also staisfy Planck data.

The plots in Fig. 4 reveal that M and g_0 values obtained are almost same for both the models

considered. Since $M_H = 360$ GeV, heavy Higgs resonance appears at 180 GeV. The green lines in Fig. 4(a,b) clearly show that for the common sets of α , β values, heavy Higgs resonance flattens near SM like condition ($\beta - \alpha \approx 90$). Plots in Fig. 4 also indicate that for low mass region, some of the g_0 values that satisfy relic density of DM are excluded from $h \rightarrow \gamma\gamma$ bounds.

5 Direct detection measurements

Direct detection of dark matter is based on the fact that DM particle interacts with the nucleon of the detecting material. The elastic scattering causes the recoil of the target nucleus or nucleon. This recoil energy is measured to determine the scattering cross-section and dark matter mass. The spin independent elastic scattering cross-section is given as

$$\sigma_{\text{SI}} \simeq \frac{m_r^2}{\pi} \left(\frac{g_{\tilde{\chi}\chi h} g_{NNh}}{m_h^2} + \frac{g_{\tilde{\chi}\chi H} g_{NNH}}{m_H^2} \right)^2. \quad (27)$$

In the above, m_r is the reduced mass $= \frac{m_\chi m_N}{m_\chi + m_N}$, where m_N is the mass of the scattering nucleon usually taken to be proton or neutron and g_{NNx} ($x = h$ or H) denotes the effective Higgs nucleon couplings expressed as [18]

$$g_{NNh} \simeq (1.217k_d^h + 0.493k_u^h) \times 10^{-3}, \quad g_{NNH} \simeq (1.217k_d^H + 0.493k_u^H) \times 10^{-3} \quad (28)$$

For THDM I, parameters k_u^h and k_d^h in Eq. 28 are given as

$$k_u^h = k_d^h = \frac{\cos \alpha}{\sin \beta} \quad k_u^H = k_d^H = \frac{\sin \alpha}{\sin \beta}. \quad (29)$$

For THDM II these parameters are

$$k_u^h = \frac{\cos \alpha}{\sin \beta} \quad k_d^h = -\frac{\sin \alpha}{\cos \beta} \quad k_u^H = \frac{\sin \alpha}{\sin \beta} \quad k_d^H = \frac{\cos \alpha}{\cos \beta}. \quad (30)$$

Using Eqs. 28 - 30 and Eq. 7, the spin independent scattering cross-section referred in Eq. 27 can be written as

$$\sigma_{\text{SI}} \simeq g_0^2 \frac{m_r^2}{\pi} \left(\frac{\sin(\beta - \alpha) g_{NNh}}{m_h^2} + \frac{\cos(\beta - \alpha) g_{NNH}}{m_H^2} \right)^2. \quad (31)$$

In Fig. 5 we present the spin independent direct detection cross-section as a function of dark matter mass. With the allowed values of the coupling parameters obtained from Fig. 4 (and Section 4), we compute the σ_{SI} given in Eq. 31. Experimental bounds on spin independent direct detection cross-section obtained from XENON100 [19] and SIMPLE [20] experiments are illustrated by solid blue line and pink line. The experimental direct detection bounds reveal that the proposed extension of type I THDM with a fermionic dark matter is almost excluded by XENON100 except the Higgs pole regions. In the SM like condition when $\sin(\beta - \alpha)$ approaches unity heavy Higgs pole disappears and only SM Higgs pole satisfies direct detection bounds achieved from Xenon100. However, for the model with type

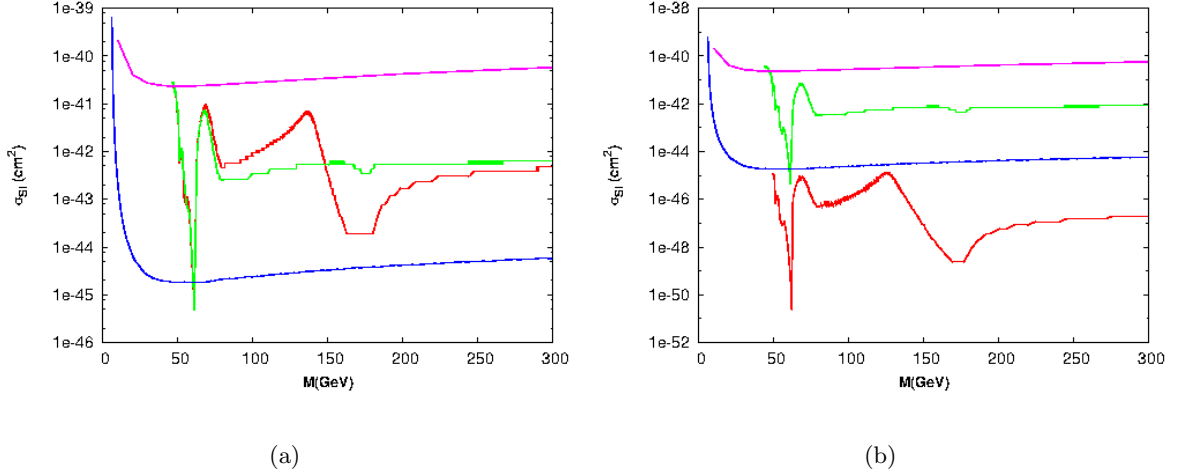


Figure 5: Spin independent scattering cross-section σ_{SI} vs dark matter mass M measured for THDM I + FDM and THDM II + FDM

II THDM and a fermionic dark matter we find that for parameter choice $\alpha = -30, \beta = 65$, the variation of σ_{SI} with M is mostly disfavoured by XENON100 data. But for the set $\alpha = 20, \beta = 65$, the σ_{SI} vs M plot in the model is allowed by XENON100 data (as also by the SIMPLE result). This is due to the fact that for parameter set I, $\beta - \alpha = 95 \simeq 90$. Hence this set is almost equivalent to SM and the σ_{SI} vs M will also be similar to the case of singlet fermion. Since for low mass dark matter, g_0 cannot exceed a certain maximum (obtained from $h \rightarrow \gamma\gamma$ results discussed in Section 3), some of the allowed results will be eliminated.

6 Discussions and Conclusions

In this work we presented a model of fermionic dark matter extending the standard model of particle physics into a two Higgs doublet model. The model conserves baryon and lepton number and baryonic and leptonic charge of the fermionic dark matter candidate is taken to be zero. This ensures the stability of the present dark matter candidate. The fermionic DM in the model can annihilate through Higgs mediated channel and couples to both the CP even Higgs particles appearing in THDM. We have explored two different types of THDMs namely THDM I and THDM II and assumed that the new found scalar boson at LHC is one of the two CP even Higgs occurring in THDM. We found the results of $h \rightarrow \gamma\gamma$ process obtained from ATLAS and CMS, set an upper bound on DM-Higgs coupling for low mass dark matter when the dark matter mass $M \leq m_h/2$ (m_h being the mass of the scalar boson discovered at LHC). Analysis of these models reveal that the fermionic dark matter in both the models (THDM I + FDM and THDM II + FDM) satisfy the observed relic abundance for a selected model parameter space (basically different couplings) that are allowed by $h \rightarrow \gamma\gamma$ process. The elastic

scattering cross-section of the dark matter off a nucleon in both the models (direct detection cross-section) are then calculated. The coupling parameter values are those allowed values required to obtain the observed relic density. A comparison of the calculated scattering cross-section for different dark matter mass with the experimental results such as XENON100 indicates that the dark matter in the THDM I + FDM is almost ruled out by XENON100 bound. But the dark matter in the other model namely THDM II + FDM is allowed by XENON100 data for a choice of parameter set within the values allowed by both $h \rightarrow \gamma\gamma$ bound and observational relic density bound. Therefore the fermionic dark matter in THDM II + FDM appears to be a viable dark matter model that can generate the observed dark matter relic density in the universe and also satisfies the most stringent bound by direct dark matter detection experiment. This also produces the allowed values of coupling parameters for the dark matter candidate.

References

- [1] P. Ade *et al.* [Planck Collaboration], arXiv:1303.5076 [astro-ph.CO].
- [2] Z. Ahmed *et al.* [CDMS Collaboration], Phys. Rev. Lett. **106**, 131302 (2011).
- [3] M. Ackermann *et al.* [LAT Collaboration], Phys. Rev. D **86**, 022002 (2012).
- [4] M. Aguilar *et al.* [AMS Collaboration], Phys. Rev. Lett. **110** 141102 (2013).
- [5] A. Abramowski *et al.* [H.E.S.S. Collaboration], Phys. Rev. Lett. **110**, 041301 (2013).
- [6] J. Albert *et al.* [MAGIC Collaboration], Astrophys. J. **674**, 1037 (2008).
- [7] J. Chang *et al.* [ATIC Collaboration], Nature **456**, 362 (2008).
- [8] V. Barger, P. Langacker, M. McCaskey, M. J. Ramsey-Musolf and G. Shaughnessy, Phys. Rev. D **77**, 035005 (2008); S. Andreas, T. Hambye and M. H. G. Tytgat, JCAP **0810**, 034 (2008); X. -G. He, T. Li, X. -Q. Li, J. Tandean and H. -C. Tsai, Phys. Lett. B **688**, 332 (2010); A. Bandyopadhyay, S. Chakraborty, A. Ghosal and D. Majumdar, JHEP **1011**, 065 (2010); S. Andreas, C. Arina, T. Hambye, F. -S. Ling and M. H. G. Tytgat, Phys. Rev. D **82**, 043522 (2010); Y. Mambrini, Phys. Rev. D **84**, 115017 (2011); E. Ma, Phys. Rev. D **73**, 077301 (2006); L. Lopez Honorez, E. Nezri, J. F. Oliver and M. H. G. Tytgat, JCAP **0702**, 028 (2007); D. Majumdar and A. Ghosal, Mod. Phys. Lett. A **23**, 2011 (2008); M. Gustafsson, E. Lundstrom, L. Bergstrom and J. Edsjo, Phys. Rev. Lett. **99**, 041301 (2007); Q. -H. Cao, E. Ma and G. Rajasekaran, Phys. Rev. D **76**, 095011 (2007); E. Lundstrom, M. Gustafsson and J. Edsjo, Phys. Rev. D **79**, 035013 (2009); E. Nezri, M. H. G. Tytgat and G. Vertongen, JCAP **0904**, 014 (2009); S. Andreas, M. H. G. Tytgat and Q. Swillens, JCAP **0904**, 004 (2009); C. Arina, F. -S. Ling and M. H. G. Tytgat, JCAP **0910**, 018 (2009); L. Lopez Honorez and C. E. Yaguna, JHEP **1009**, 046 (2010); D. Borah and J. M. Cline, Phys. Rev. D **86**, 055001 (2012).

- [9] G. C. Branco, P. M. Ferreira, L. Lavoura, M. N. Rebelo, M. Sher, and J. Silva, arXiv:1106.0034.
- [10] Y. G. Kim and K. Y. Lee, Phys. Rev. D **75**, 115012 (2007).
- [11] J. F. Gunion, H. E. Haber, G. L. Kane, and S. Dawson, Front. Phys. **80** 1 (2000).
- [12] G. Aad *et al.* [ATLAS Collaboration], Phys. Lett. B **716**, 1 (2012).
- [13] S. Chatrchyan *et al.* [CMS Collaboration], Phys. Lett. B **716**, 30 (2012).
- [14] P. M. Ferreira, R. Santos, M. Sher, J. P. Silva, Phys. Rev. D **85**, 077703 (2012).
- [15] ATLAS-CONF-2013-012; CMS-HIG-13-001.
- [16] P. M. Ferreira, Rui Santos, Marc Sher, Joo P. Silva arXiv:1305.4587 (2013).
- [17] E.W. Kolb and M. Turner, *The Early Universe* (Westview Press, Boulder, 1990).
- [18] X. -G. He, T. Li, X. -Q. Li, J. Tandean and Ho-C. Tsai, Phys. Rev. D **79**, 023521 (2009).
- [19] E. Aprile *et al.* [XENON100 Collaboration], Phys. Rev. Lett. **109**, 181301 (2012).
- [20] M. Felizardo *et al.* [SIMPLE Collaboration], Phys. Rev. Lett. **105**, 211301 (2010).